RESEARCH

Compound fermentation supernatants of antagonistic bacteria control *Rhizoctonia cerealis* and promote wheat growth

Yanjie Yi[1,3]*, Yang Liu[1,3], Pengyu Luan[1,3], Zhipeng Hou[1,3], Yanhui Yang[1,3], Ruifang Li[1,3], Zhenpu Liang[2], Xiaoxia Zhang[2] and Shulei Liu[1,3]

Abstract

Background: Wheat sheath blight, caused by *Rhizoctonia cerealis*, is a popular fungal disease that causes serious harm to wheat production. Biological control can offer the safe and effective method to control wheat diseases.

Results: In this study, antagonistic bacteria XZ20-1 and XZ38-3 were isolated and identified as *Bacillus amyloliquefaciens* and *Bacillus velezensis*, respectively, and all produced cellulase, protease, amylase and siderophore. To improve antifungal activity, fermentation supernatants of antagonistic bacteria *Pseudomonas fluorescens* RB5 (previously isolated and stored in the laboratory), *B. amyloliquefaciensns* XZ20-1 and *B. velezensis* XZ38-3 were combined and the optimal compound ratio (2:6:4) was quickly screened out through the improved triangle coordinate diagram method. The inhibition rate of compound fermentation supernatants (CFS) reached 61.01%, which was 22.51, 17.05 and 21.42% higher than that of single strain, respectively. The further stability analysis showed that compound fermentation supernatants were relatively stable to pH, temperature, ultraviolet and light. Effect of CFS on pathogen cells through fluorescent microscopy using different stains revealed the mechanism, which CFS can cause cell membrane permeability changed, accumulation of ROS and DNA fragmentation. In the pot experiments, the control efficacy of CFS was 83.05%. Moreover, plant height, root length and fresh weight, chlorophyll and soluble protein of wheat seedlings in CFS treatment groups were more than those in the control group.

Conclusions: This work screened out the optimal compound ratio of fermentation supernatants by the improved triangular coordinate diagram method firstly and revealed the action mechanism and provides an effective microbial agent for controlling *R. cerealis* and promoting wheat growth.

Keywords: *Rhizoctonia cerealis*, Wheat sheath blight, Compound fermentation supernatants, Antifungal activity, Action mechanism, Growth promotion

Background

Wheat is the dominant cereal crop in the world. Approximately 85% of humans get most of their basic calories and protein from wheat (Nassar et al. 2020). Wheat sheath blight (also known as wheat sharp eyespot), caused by

Rhizoctonia cerealis, is one of the popular fungal diseases that causes serious harm to global wheat production in recent decades (Ren et al. 2020). *R. cerealis* can infect the roots and basal stems at any time during the wheat growing season and in turn can devastate the transport of tissues in stems of wheat and obstruct transportation of nutrition substances (Su et al. 2020). With the increased planting of high-yielding varieties and the increased use of fertilization and irrigation, wheat sheath blight become a serious disease of wheat in China, and the area where the sheath blight occurs has increased yearly (Peng

*Correspondence: yiyanjie@haut.edu.cn

[1] School of Biological Engineering, Henan University of Technology, Zhengzhou 450001, China
Full list of author information is available at the end of the article

Yi et al. Egyptian Journal of Biological Pest Control   (2022) 32:121

Page 2 of 14

et al. 2014). In particular, within the last two decades, the implementation of straw return in China promoted the outbreak of wheat sheath blight (Su et al. 2021). The breeding of wheat varieties with resistance to sheath blight would seem to be the promising way to control this disease, but highly resistant varieties are still insufficient. Chemical pesticides have been developed to prevent the serious occurrence of diseases and are also the most important means of prevention nowadays. However, long-term use of chemical pesticides would cause serious consequences, such as severe toxicity, high residue and environmental pollution and other deficiencies (Nguyen et al. 2020).

Biocontrol agents have many advantages such as being residue-free, pollution-free and environment-friendly, which can offer a safe and effective method to control wheat diseases (Lim et al. 2017). In recent years, biological control agents have been paid more attention. The global biocontrol market was assessed as $1.5 billion in 2016, represented only 2% of the chemical pesticide market, and is expected to reach $3.67 billion in the world by 2022 (Helepciuc and Todor 2021). *Bacillus*, widely existing in nature, has a broad antifungal spectrum and plant growth-promotion properties which facilitate the formulation into biocontrol agents (Yi et al. 2018). It is reported that *B. cereus* 0–9 could reduce the disease incidence of wheat sheath blight (Xu et al. 2014). *Bacillus* could produce antimicrobial proteins that altered the cell wall structure of mycelium and inhibit the mycelial growth of *R. cerealis* (Zhang et al. 2020).

Fermentation supernatants or active substances of antagonistic strain can be further developed into antimicrobial agents for better application in biological control. Combining different antagonistic bacteria may improve the antifungal effect (Hasan et al. 2020). Different active substances produced by different antagonistic bacteria may lead to an increase in antimicrobial diversity, thereby affecting the invasion of other species (Niu et al. 2020). For the combination of multi-components, the methods commonly used are proportional method, orthogonal design method, triangular coordinate diagram method, uniform design, etc. Compared with the orthogonal design method and the uniform design method, the triangular coordinate diagram can more intuitively and clearly express the law of the properties of the compound changing with the ratio. Although many coordinate points are constructed in the triangle, only several representative points are selected at the beginning, which can narrow the range of the best ratio. In this range, the best ratio of the three substances can be obtained (Sofue et al. 1997). The triangular coordinate diagram method is rapid and simple, can improve the efficiency of screening different formulations, and has good scientific and practical

properties, but its application in the combination of strains has not been reported.

It is of great significance to isolate antagonistic bacteria with high resistance to wheat sheath blight and improve their antifungal ability. However, biocontrol agents are not sufficient, so effective biocontrol resources and agents are urgently needed to be developed. In the present study, bacteria XZ20-1 and XZ38-3 antagonistic to *R. cerealis* were isolated and identified as *B. amyloliquefaciens* and *B. velezensis*, respectively, and their bioactive substances were detected. The optimal compound ratio of fermentation supernatants of antagonistic bacteria *Pseudomonas fluorescens* RB5 (previously isolated and stored in the laboratory), *B. amyloliquefaciens* XZ20-1 and *B. velezensis* XZ38-3 was quickly screened out by the improved triangular coordinate diagram method. Stability and action mechanism of compound fermentation supernatant (CFS) were analyzed, and the biocontrol efficacy for wheat sheath blight and plant growth-promotion properties of CFS were further evaluated for exploiting the environmentally friendly control agents against wheat sheath blight.

Methods

Isolation, purification and screening of antagonistic bacteria

Soil samples used for isolating the antagonistic bacteria were provided by Dr. Yu Shi of the Institute of Soil Science, Chinese Academy of Sciences. The biocontrol bacteria *Pseudomonas fluorescens* RB5 isolated from soil and pathogenic fungi *R. cerealis* was deposited in the laboratory.

Each soil sample was serially diluted to 10^8 times with sterile distilled water. Subsequently, 100 μl of the most diluted soil re-suspension was spread on LB medium plates and incubated at 37 °C for 48 h. The colonies with different morphology were selected for purifying and testing their antifungal activity by plate confrontation assay. Disk of *R. cerealis* with 6 mm diameter was placed at the center on the PDA medium, and four different purified bacteria were inoculated equidistantly with the distance of 3 cm from the center. Plate only inoculating with *R. cerealis* was set as control. The plates were incubated at 28 °C under dark conditions for seven days, and inhibiting effect of antagonistic bacteria on pathogen was determined as described by Pan et al. (2021). Each experiment was repeated three times. Antagonistic strains were preserved in 40% glycerol at −80 °C for further processing.

Identification of antagonistic bacteria

Antagonistic bacteria were cultured on LB medium plate, placed at 28 °C for 24 h, and colony characteristics, such

Yi *et al. Egyptian Journal of Biological Pest Control*   (2022) 32:121

Page 3 of 14

as color, morphology and transparency, were directly observed. The physiological and biochemical tests of antagonistic bacteria were carried out using universal methods (Guerrero 2001).

Genomic DNA of antagonistic bacteria was extracted by the CTAB method (Guo et al. 2000). The bacterial universal primer pair, 27F (5′-AGAGTTTGATCCTGG CTCAG-3′) and 1492R (5′-GGTTACCTTGTTACGACT T-3′) were used to amplify the 16S rDNA gene (El-Helw et al. 2019). The gyrB gene sequence was identified using the gyrB F (5′-TTATCTACGACCTTAGACG-3′) and gyrB R (5′-TAAATTGAAGTCTTCTCCG-3′) primers (Liu et al. 2013). PCR was performed using a Taq DNA polymerase kit (Sangon Biotech Co., Ltd., Shanghai, China) in 25 μl reactions. The PCR program was the initial denaturation step at 94 °C for 4 min, then 30 cycles of 94 °C for 30 s, 50 °C for 30 s, and 72 °C for 90 s, followed by a final extension step at 72 °C for 10 min. PCR products were sent to Sangon Biotech Co., Ltd., (Shanghai, China) for sequencing. The DNA sequences were

To improve antifungal activity, the improved triangle coordinate diagram method was used to screen the optimal compound ratio of fermentation supernatants of three antagonistic bacteria. The outermost binary combination was removed and reduced to 55 ratios, so that each locus becomes the ternary combination system. While the screening density was increased and then compared to the effect of equiproportional combination of the two strains was compensate for the use of the outermost binary combination system to narrow the range of optimal ratios. A few representative points were selected according to the usual rules, namely 1, 5, 7, 10, 13, 17, 20, 22, 25, 28, 31, 34, 38, 41, 44, 46, 49, 52 and 55, and then the area where the better combination formulation located was determined according to the results of the test index. Each treatment was repeated four times, and the test was repeated thrice.

The mycelial growth rate method was used to determine the inhibition rate of the fermentation supernatants against *R. cerealis* (Tian et al. 2021). Inhibition rate is calculated according to the following formula:

$$\text{Inhibition rate}(\%) = \frac{\text{The mycelial radial diameter of the pathogen in the control group} - \text{The mycelial radial growth diameter of the pathogen in the treatment group}}{\text{The mycelial radial growth diameter of the pathogen in the control group}} \times 100$$

blasted in the GenBank (Bethesda, MD, USA; http:// www.ncbi.nlm.nih.gov/Blast). The 16S rDNA sequences of XZ20-1 and XZ38-3 have been deposited in the GenBank database with the accession numbers MZ646067.1 and MZ646068.1, respectively. The DNA sequences were analyzed by Clustal 2.0, and the phylogenetic trees were constructed by MEGA 7.0 software. The reliability of trees was evaluated by producing 1 000 bootstrap replicates (Kumar et al. 2016).

Detection of bioactive substances produced by antagonistic bacteria
Bioactive substance produced by antagonistic bacteria was detected**.** Protease, cellulase and siderophore were detected with the protocols of Ben Khedher et al. (2021). Amylase was determined referring to the method of Dash et al. (2015).

Determination of optimal compound ratio of fermentation supernatants of three antagonistic bacteria
The antagonistic bacteria were inoculated in LB liquid medium and incubated at 35 °C, 160 r/min for 12 h, and the bacterial culture was inoculated in LB medium with the inoculation volume of 3% and incubated at 36 °C, 160 r/min for 48 h, then centrifuged at 12,000 r/min for 15 min and filtered with 0.22-μm sterile filter membrane for obtaining fermentation supernatants.

Tests for stability of antifungal activity of CFS
Thermal treatment: CFS were divided into 10 equal parts treated under 4, 20, 30, 40, 50, 60, 70, 80, 90 and 100 °C with 2 h and then cooled to room temperature, and 20 °C treatment was set as control (Zhao et al. 2017). Acid–base treatment: CFS were divided into 7 equal parts, and every part was adjusted the pH to 1, 3, 5, 7, 9, 11 and 13 with 1 mol/l HCl and 1 mol/l NaOH, respectively, and pH 7 treatment was set as control (Hasani et al. 2018). Ultraviolet light treatment: CFS were divided into 10 equal parts and placed at a distance of 30 cm under a 20 W UV lamp for 15, 30, 45, 60, 75, 90, 105, 120, 135 and 150 min, respectively, and the untreated CFS were set as control (Zhao et al. 2017); light treatment: CFS were divided into 7 equal parts and placed in the illumination incubator (4000 lx) for light irradiation with 0, 2, 4, 6, 8, 10 and 12 h (Yi et al. 2022a). Each test was repeated three times. The mycelial growth rate method was used to determine the inhibition rate of the CFS under different treatments (Zhao et al. 2017).

Action mechanism investigation of CFS on *R. cerealis*
The mycelial cells treated with CFS were stained with trypan blue stain solution, propidium iodide (PI), 2,7-dichlorofluorescein diacetate (DCFH-DA) and 4′,6-diamidino-2-phenylindole (DAPI) for detecting cell membrane permeability, reactive oxygen species

accumulation and DNA damage (Li et al. 2021). The mycelia were cultured in potato dextrose broth (PDB) containing CFS (300 µl/ml) for 24 h. Sterile water treatments were set as control. The mycelium was washed with phosphate buffer solution (PBS, 0.2 mM, pH 7.4) for 4 times. For trypan blue staining, mycelia cells were stained with 0.04% trypan blue stain solution at 28 °C in the dark for 4 min. For PI staining, mycelia cells were stained with 10 µg/ml PI solution at 28 °C in the dark for 15 min. For DCFH-DA staining, mycelia cells were stained with 10 µM DCFH-DA solution at 28 °C in the dark for 20 min. For DAPI staining, mycelia cells were stained with 10 µg/ml DAPI solution at 28 °C in the dark for 20 min. Then it washed with PBS for 4 times to decolorize. The stained hyphae were visualized through a fluorescence microscope with an excitation of 364 nm and emission of 454 nm. Each experiment was repeated three times.

Detection of biocontrol effect of CFS for wheat sheath blight

Seeds of wheat CV. Jimai 22 were surface-disinfected with 1% (w/v) NaClO and rinsed three times using sterile distilled water, treated with LB medium (control), the fermentation supernatants of RB5, XZ20-1, XZ38-3 and CFS, then sown in soil (uniform particle size, 60% moisture content). Twenty seeds were sown in each pot with the diameter of 15 cm and then grew in plant growth chamber at 22 ± 3 °C, with the RH of 70 ± 5% and the light/dark (L:D) ratio of 14:10 h. Every pot was poured into 20 ml *R. cerealis* suspension ($OD_{430} = 0.45$). Each test was repeated three times.

Disease incidences were recorded at 14 days after emergence according to the scale from 0 to 7 as follows: 0, no lesions; 1, lesions on the sheath but not on the stem; 3, lesions covering < 50% of the stem circumference; 5, lesions covering > 50% of the stem circumference, accompanied by plant wilt or head blight; and 7, lodging and dying. Disease index and control efficacy were calculated according to the method of Zhang et al. (2017).

$$\text{Disease index(\%)} = \frac{\sum (\text{The number of diseased plants with a certain index value} \times \text{Index value})}{\text{Total number of plants investigated} \times \text{Highest disease index}} \times 100$$

$$\text{Control efficacy(\%)} = \frac{\text{Disease index in the control group} - \text{Disease index in the treatment group}}{\text{Disease index in the control group}} \times 100$$

Growth promotion effects of CFS on wheat seedlings

Seeds of wheat CV. Jimai 22 after surface-disinfected were soaked with LB medium (control), the fermentation supernatants of RB5, XZ20-1, XZ38-3 and CFS for 30 min, and then sown in soil (uniform particle size, 60% moisture content) with 25 seeds each pot (10 cm diameter) (Zhang et al. 2017). Wheat seedlings were grown in plant growth chamber at 22 ± 3 °C, with the RH of 70 ± 5% and the L:D ratio of 14:10 h. Each experiment was repeated three times. Plant height, root length, fresh weight and dry weight were measured at 14 days after emergence.

Detection of chlorophyll, carotenoids and soluble protein in wheat seedlings

Leaves of wheat were cut and ground with 95% (v/v) ethanol, quartz sand and calcium carbonate to extract chlorophyll and carotenoids, which were measured under the levels of absorbance at 665 nm, 649 nm and 470 nm using a spectrophotometer (UV-1100, Shanghai Meipuda Instrument Co., Ltd.) as described by Lichtenthaler and Wellburn (1983). Soluble protein of wheat seedlings was measured according to the method of Carvalho et al. (2019). Each experiment was repeated three times. Total reducing sugars were analyzed by the 3, 5 dinitrosalicylic acid method (Miller 1959), and the total soluble protein content was measured according to Carvalho et al. (2019).

Data analysis

Statistical variance of the experimental data between all groups was analyzed using SPSS 20.0, and the significance of the differences in the experimental data was analyzed using Duncan's new complex polar difference method as described by Yi et al. (2022b). The significant differences were set as $P < 0.05$.

Results

Isolation and identification of antagonistic bacteria

A total of 180 bacterial strains were isolated from the soil. All of the isolates were screened for controlling *R. cerealis* with the inhibition zone method. Two strains XZ20-1 and XZ38-3 and their fermentation supernatants showed a significant inhibition activity against *R. cerealis*.

Colony XZ20-1 showed white, spherical, opaque, neat edges, no wrinkles, moist surface, smooth and easy to pick up (Fig. 1a). Colony XZ38-3 showed white,

Yi *et al. Egyptian Journal of Biological Pest Control*   (2022) 32:121

Page 5 of 14
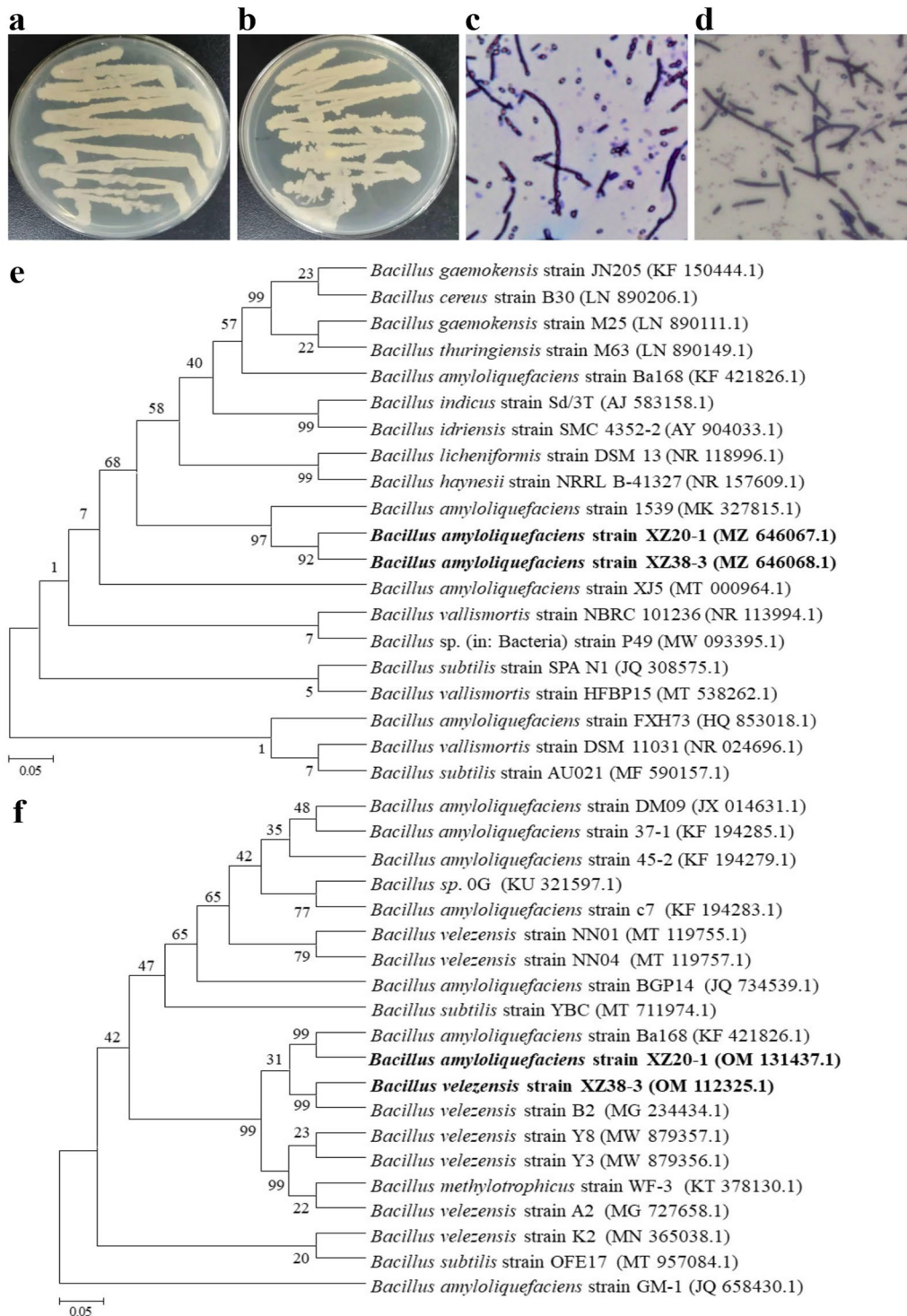
Fig. 1 Morphological characteristic and phylogenetic trees of strains XZ20-1 and XZ38-3. **a** Colony morphology of XZ20-1; **b** Colony morphology of XZ38-3; **c** The bacterial cell of XZ20-1 (Gram stain); **d** The bacterial cell of XZ38-3 (Gram stain); **e** Phylogenetic tree of XZ20-1 and XZ38-3 based on the sequences of 16 S rDNA gene; **f** Phylogenetic tree of XZ20-1 and XZ38-3 based on the sequences of gyrB gene

Yi *et al. Egyptian Journal of Biological Pest Control*   (2022) 32:121

Page 6 of 14

spherical, opaque, neat edges, wrinkles, moist surface, not smooth and easy to pick up (Fig. 1b). Both antagonistic strains XZ20-1 and XZ38-3 were Gram-positive bacteria (Fig. 1c, d).

Physiological and biochemical examination showed both strains XZ20-1 and XZ38-3 could not decompose lactose and glucose, and methyl red reaction, V. P. test and citratio utilization test were all negative, while the starch hydrolysis, indole reaction, nitrate reduction reaction and contact enzyme reaction were all positive.

Based on 16S rDNA sequence alignment and the phylogenetic tree, XZ20-1 and XZ38-3 were highly similar to *B. amyloliquefaciens* (Fig. 1e). As shown in the phylogenetic trees constructed using the gyrB gene sequence (Fig. 1f), XZ20-1 had 99% similarity with *B. amyloliquefaciens* Ba168 (KF421826.1) and XZ38-3 had 99% similarity with *B. velezensis* strain B2 (MG234434.1). Considering morphological characteristics, physical and chemical analysis and molecular identification, the strain XZ20-1 was identified as *B. amyloliquefaciens* and XZ38-3 was identified as *B. velezensis*.
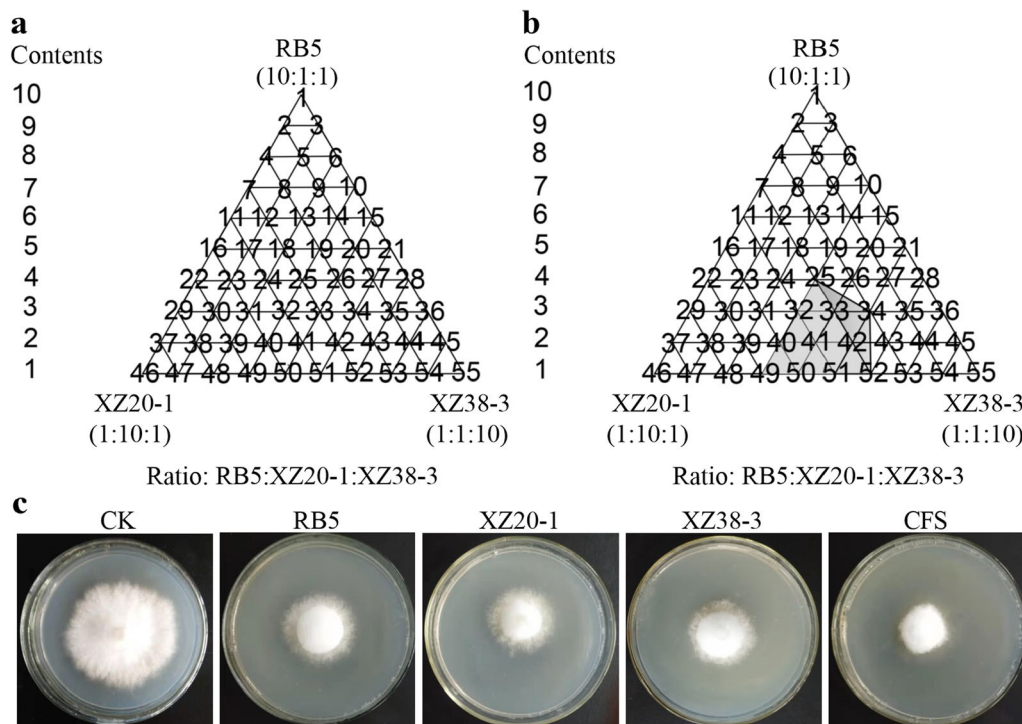
Bioactive substance produced by antagonistic bacteria

The bioactive substance of *B. amyloliquefaciens* XZ20-1, *B. velezensis* XZ38-3 and *P. fluorescens* RB5 was tested for bioactive substance. Strains XZ20-1, XZ38-3 and RB5 produced transparent circles on four identification media, indicating that all strains produced cellulase, protease, amylase and siderophore. However, XZ20-1 produced more amylase, XZ38-3 produced more cellulase and RB5 produced more siderophore (Fig. 2).

To improve antifungal activity, fermentation supernatants of *B. amyloliquefaciens* XZ20-1, *B. velezensis* XZ38-3 and *P. fluorescens* RB5 were combined, and the improved triangle coordinate diagram method was used for determining the optimal compound ratio. The fermentation supernatants of antagonistic bacteria RB5, XZ20-1 and XZ38-3 were set as three variables (Fig. 3a). Fermentation supernatants of antagonistic bacteria RB5, XZ20-1 and XZ38-3 were combined according to the ratios represented by points 1, 5, 7, 10, 13, 17, 20, 22, 25, 28, 31, 34, 38, 41, 44, 46, 49, 52 and 55 in the improved triangular coordinate diagram.

The ratio of each group and their inhibition rates against *R. cerealis* are shown in Table 1. Inhibition rates of the CFS were improved compared with that of the

Fig. 2 Detection of bioactive substance from *Bacillus amyloliquefaciens* XZ20-1, *Bacillus velezensis* XZ38-3 and *Pseudomonas fluorescens* RB5
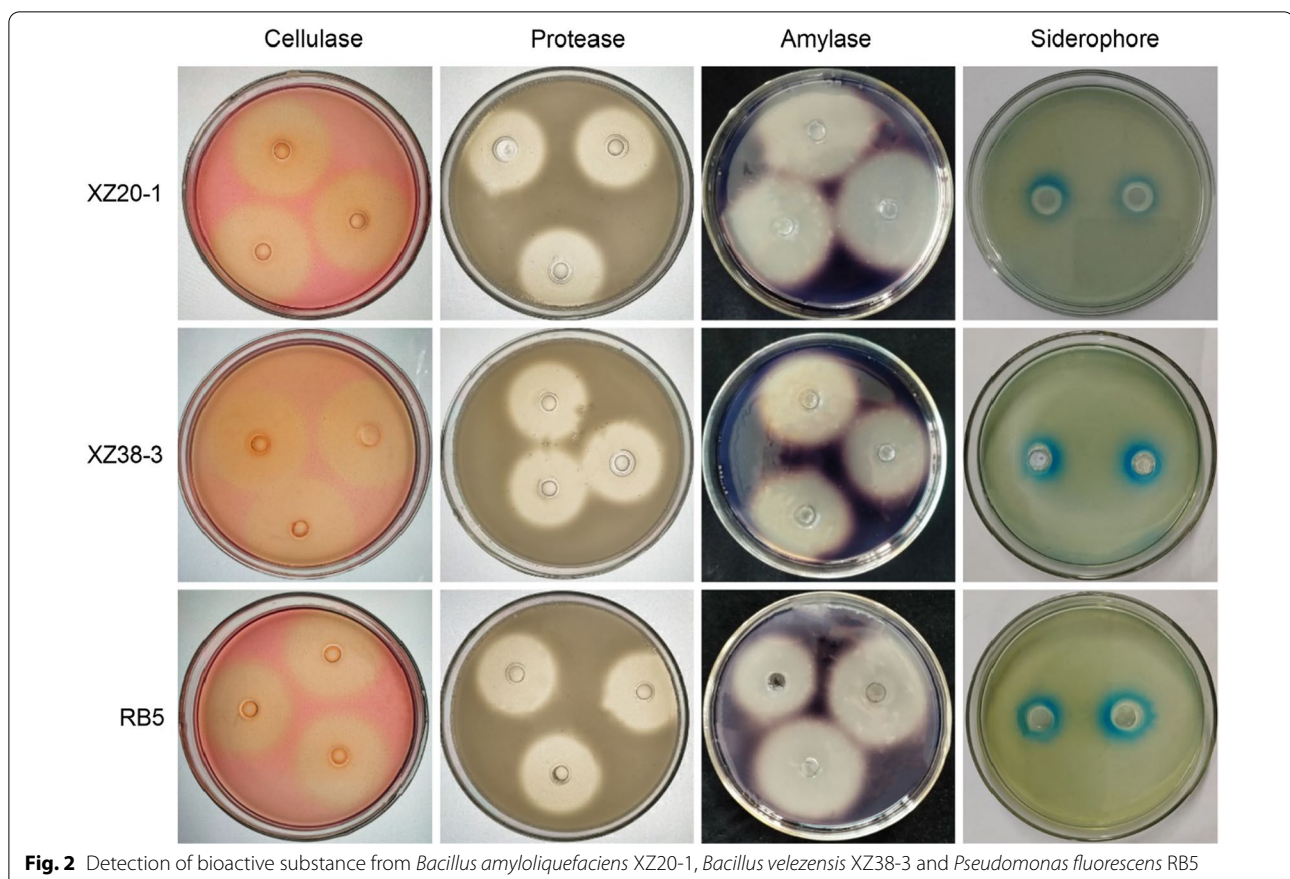
Fig. 3 Ratio of three strains and inhibition effects of fermentation supernatants. **a** Ratio of strains in the improved triangular coordinate diagram; **b** The optimal compound ratios shown in the triangular coordinate diagram; **c** Inhibition effects of fermentation supernatants of strains on *Rhizoctonia cerealis*

single strain fermentation supernatants, and the inhibition rates of numbers 25, 34, 49 and 52 were 59.88, 59.85, 59.94 and 60.05%, respectively. It is inferred that the optimal compound ratio was concentrated in the triangular region of 25, 34, 49 and 52 (Fig. 3b). It indicated that the antifungal substances produced by the fermentation supernatants of the three antagonistic bacteria may complement each other.

According to points 32, 33, 40, 42, 50 and 51 selected from the shaded area in (Fig. 3b), the fermentation supernatants were combined, and the inhibition rates were calculated (Table 2). Among them, the best inhibition rate with the compound ratio at point 40 reached 61.01% (Fig. 3c), which was 22.51, 17.05 and 21.42% higher than that of single strain RB5, XZ20-1 and XZ38-3, respectively. Therefore, the compound ratio (2:6:4) of the fermentation supernatants at point 40 was chosen as the optimal compound ratio of three strains RB5, XZ20-1 and XZ38-3.

Stability analysis of the antifungal activity of CFS
When the CFS were treated under different temperatures (4–90 °C), there was nonsignificant difference in antifungal activities than the control (room temperature 20 °C treatment), but when the CFS were treated with 100 °C, the antifungal activity decreased and the inhibition rate was 55.54%, which was significantly different than the control. The results indicated that the CFS had a good activity stability after treatment from 4 to 90 °C (Fig. 4a), whereas it was not stable to 100 °C.

The antifungal activity of the CFS treated with different pH was relatively stable at pH 3–9. Under strong acid and strong alkaline treatments, the inhibition rates of the CFS against *R. cerealis* were significantly different with the control group, and the inhibition rate was reduced to 51.74% at pH = 1 and 49.86% at pH = 13, which indicated that the CFS had no better tolerance to strong acid and strong alkaline, and the suitable pH was 3–9 (Fig. 4b).

The antifungal activity of CFS was slightly reduced with the extension of the irradiation treatment time after different times under ultraviolet light (Fig. 4c), but the inhibition rates were all greater than 55%. It showed that the CFS had good activity stability to UV light irradiation for a long time.

Compared with the control group, the antifungal activity of CFS changed slightly under different light irradiation treatments. When the time of light irradiation was less than 4 h, the inhibition rates were less affected. When the light irradiation time is longer than 6 h, the inhibition rates slightly decreased but are still greater than 57%. This indicated the CFS has good stability to light (Fig. 4d).

Yi *et al. Egyptian Journal of Biological Pest Control* (2022) 32:121

Page 8 of 14

Table 1 Ratio of each group and their inhibition rates against *Rhizoctonia cerealis*

Number	RB5:XZ20-1:XZ38-3	Diameter of growth (mm)	Inhibition rate (%)
1	10:1:1	40.43 ± 0.28	42.72 ± 0.70[e]
5	8:2:2	36.60 ± 0.51	49.28 ± 0.96[d]
7	7:4:1	35.02 ± 0.56	51.99 ± 1.29[cd]
10	7:1:4	36.53 ± 1.11	49.39 ± 1.91[d]
13	6:3:3	34.76 ± 0.41	52.43 ± 0.79[c]
17	5:5:2	34.86 ± 0.56	52.26 ± 0.97[cd]
20	5:2:5	35.16 ± 0.36	51.75 ± 0.45[cd]
22	4:7:1	34.70 ± 1.33	53.54 ± 2.28[c]
25	1:1:1	30.42 ± 1.37	59.88 ± 2.35[a]
28	4:1:7	32.72 ± 1.27	55.92 ± 2.18[b]
31	3:6:3	31.56 ± 1.11	57.92 ± 1.90[ab]
34	3:3:6	30.43 ± 1.00	59.85 ± 1.71[a]
38	2:8:2	31.89 ± 1.74	57.36 ± 2.99[ab]
41	2:5:5	30.92 ± 0.40	59.02 ± 0.68[ab]
44	2:2:8	32.80 ± 1.24	55.79 ± 2.13[b]
46	1:10:1	33.33 ± 0.40	54.89 ± 0.69[bc]
49	1:7:4	30.38 ± 1.11	59.94 ± 1.89[a]
52	1:4:7	30.32 ± 0.49	60.05 ± 0.85[a]
55	1:1:10	34.12 ± 0.35	53.53 ± 0.60[c]
A	1:1:0	39.10 ± 0.37	44.99 ± 0.28[e]
B	1:0:1	40.64 ± 0.67	42.36 ± 1.16[e]
C	0:1:1	38.85 ± 0.63	45.47 ± 1.42[e]
XZ20-1		39.70 ± 0.55	43.96 ± 1.53
XZ38-3		42.25 ± 0.72	39.59 ± 1.82
RB5		42.89 ± 0.24	38.50 ± 1.43
CK		65.36 ± 0.20	

Different letters in the same column indicate significant differences ($P < 0.05$); A, B, C represented two antagonistic bacterial fermentation supernatants combined in equal proportions

Table 2 Preferred compound ratios and inhibition rates

Number	RB5:XZ20-1:XZ38-3	Diameter of growth (mm)	Inhibition rate (%)
CK		69.05 ± 0.97	–
32	3:5:4	32.90 ± 0.50	58.26 ± 0.80[c]
33	3:4:5	31.72 ± 0.77	60.16 ± 1.24[b]
40	2:6:4	31.19 ± 0.12	61.01 ± 0.20[a]
42	2:4:6	32.37 ± 0.54	59.12 ± 0.87[bc]
50	1:6:5	32.56 ± 0.48	58.80 ± 0.77[bc]
51	1:5:6	32.36 ± 0.01	59.13 ± 0.01[bc]

Different letters in the same column indicate significant differences ($P < 0.05$)

Action mechanism analysis of CFS against *R. cerealis*

Trypan blue staining is usually used to identify dead cells in tissue and cell culture, so we used trypan blue staining to observe the mycelial cell death after CFS treatment.

From (Fig. 5a), it can be seen that mycelial cell in the control group with trypan blue staining was more even and light blue staining, but in the treatment group, dark blue staining was presented in mycelium cell, especially in mycelial ball which indicated cell damage. These results showed that the mycelia in the control group could exclude and prevent trypan blue from entering the cells. However, mycelia cells were destroyed and cell membrane integrity was damaged by the CFS resulted in trypan blue entering the cells, so the cells are dyed to blue or dark blue. It indicates that CFS can cause cell death of *R. cerealis*.

Cell membranes damaged in mycelia can emit red fluorescence after PI stained under fluorescence microscopy. CFS can cause mycelial expansion of *R. cerealis*, which may endanger the integrity of mycelial cell membrane. As shown in (Fig. 5b), the mycelia treated with CFS exhibited red fluorescence, but the red fluorescence of the mycelia in the control group is very weak or even not appear. These results indicated that CFS could destroy the integrity of the cell membrane of *R. cerealis* mycelium.

After CFS treatment, the mycelia of *R. cerealis* may produce a series of defense-related reactions, among which oxygen species (ROS) levels is one of the important reaction mechanisms. As shown in (Fig. 5c), the green fluorescence of *R. cerealis* mycelium treated with CFS was significantly higher than that in control group, which indicates that CFS can increase ROS accumulation in the mycelia.

DAPI staining was used to evaluate DNA damage. Intensity of blue fluorescence in *R. cerealis* treated with CFS was stronger than that of the control group, indicating that CFS can cause DNA damage to the mycelium and inhibit the mycelium development (Fig. 5d).

Biocontrol efficacy of CFS for wheat sheath blight

The disease index and control efficacy are shown in (Fig. 6a, Table 3). The disease indexes of the control group were 49.68%, and among them, the most serious disease level 7 was 21.11%. With CFS and different fermentation supernatants treatment, the disease indexes of CFS, RB5, XZ20-1 and XZ38-3 were 8.41, 27.75, 19.84 and 24.60%, respectively. The most serious disease level 7 in the CFS treatment group was 2.22%, which was 18.89% lower than that in the control group. The control efficacy of CFS and fermentation supernatant of RB5, XZ20-1, XZ38-3 were 83.05, 44.14, 60.03 and 50.53%, respectively. The results indicated that the control efficacy of CFS was significantly improved compared with that of the single strain.

Evaluation of wheat growth-promotion properties of CFS

After wheat seedlings grew for 14 days (Fig. 6b), wheat plant height, root length and fresh weight in RB5 and

Yi *et al. Egyptian Journal of Biological Pest Control*   (2022) 32:121

Page 9 of 14
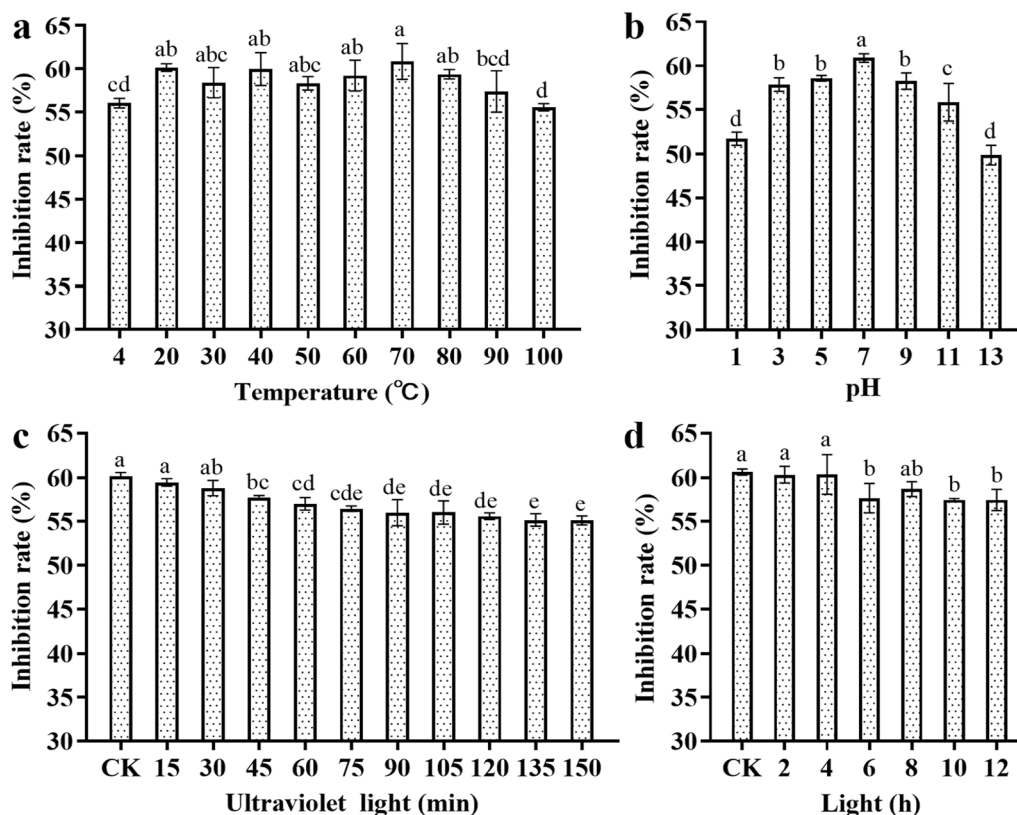
Fig. 4 Inhibition rates of compound fermentation supernatants (CFS) under different treatments. **a** Temperature; **b** pH; **c** Ultraviolet light; **d** Light. Different letters in the figures indicate significant differences ($P < 0.05$)

CFS treatment groups were more than those in the control group. The results indicated that CFS could promote wheat growth (Fig. 6c, d). The contents of chlorophyll a in wheat leaves in the CFS treatment group were more than those in the control group, RB5 and XZ38-3 treatment groups. The contents of soluble protein in the CFS treatment group were also significantly more than those in the control group, RB5 and XZ20-1 treatment groups, and the protein content was 2.36 times more than that in the control group. However, there was non-significant change in chlorophyll b and carotenoid contents (Fig. 6e, f), which indicated that CFS could promote the synthesis of chlorophyll and soluble protein in wheat leaves, thereby improving the conversion rate of light energy and promoting the growth of wheat.

Discussion

Beneficial bacteria for biological control are a safe and effective method, which can reduce the high residue and environmental pollution caused by chemical pesticides (Hasan et al. 2020). The present study aimed to find beneficial bacteria against *R. cerealis* and improve antifungal activity. Antagonistic bacteria XZ20-1 and

XZ38-3 were screened and showed a good inhibition effect against *R. cerealis. Bacillus* can produce many kinds of active substances during the fermentation metabolism, including bacteriocins, antibiotics, hydrolytic enzymes and some growth factors, which have a great practical value (WoldemariamYohannes et al. 2020). *P. fluorescens* RB5 isolated in the laboratory previously can produce siderophores. It can dissolve iron which is not directly available to plants, thus promoting iron availability for the growth of plants (Ma et al. 2016). Siderophores have received great attention in plants, biotechnology and environmental research due to their high affinity and specificity for Fe^{3+} (Kulišová et al. 2021). Combination of active substances from different strains may produce resistance gain, which is consistent with the conclusions that metabolic product of one microbe may be beneficial to another or show complementary advantages (Hu et al. 2019). To date, few methods have been developed for rapidly screening the optimal compound ratio. Through the triangular coordinate diagram method, three variables are chosen and the total number 12 of the three substances added together is determined. In this study, two antagonistic

Yi *et al. Egyptian Journal of Biological Pest Control*   (2022) 32:121
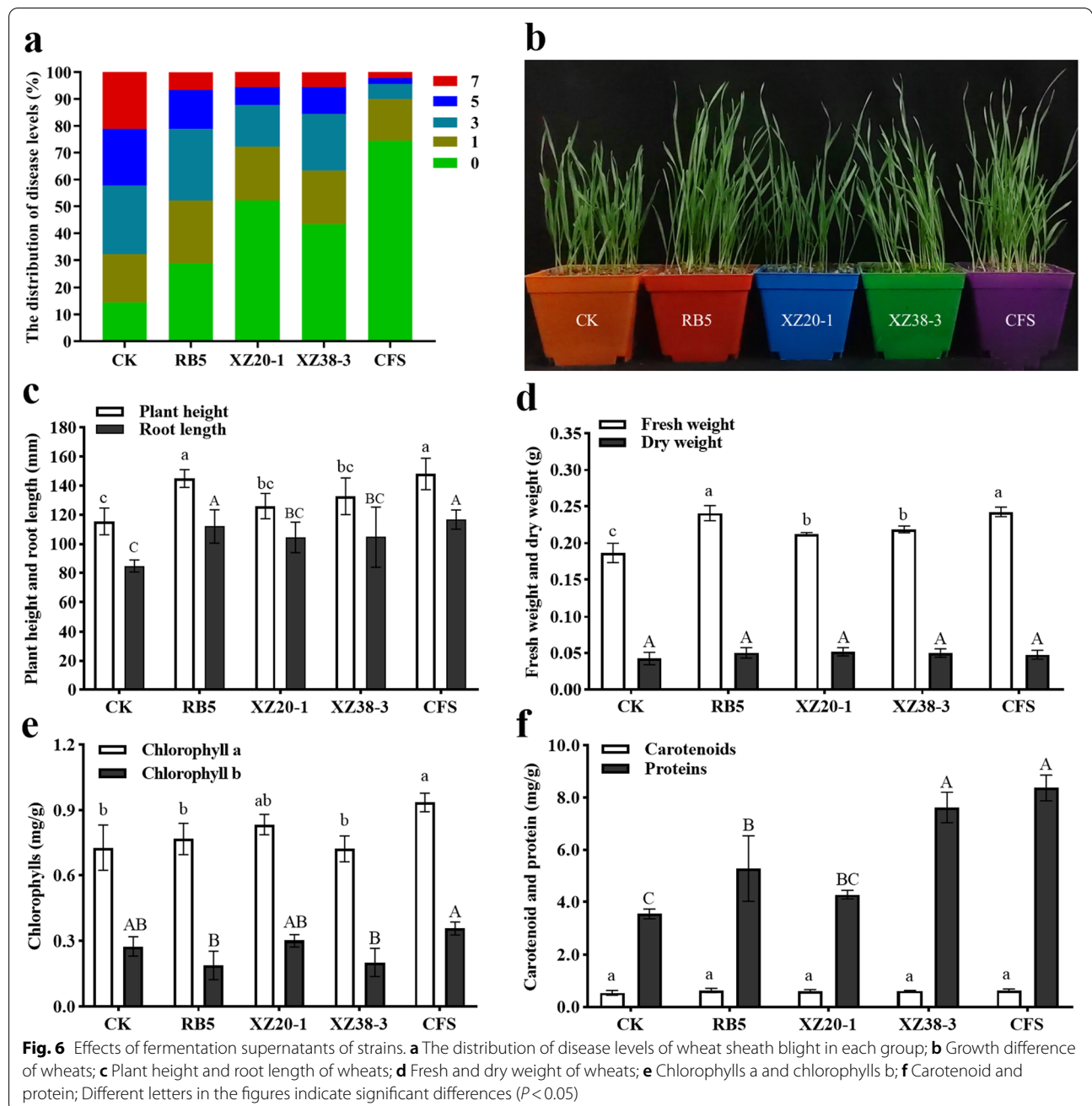
Page 10 of 14
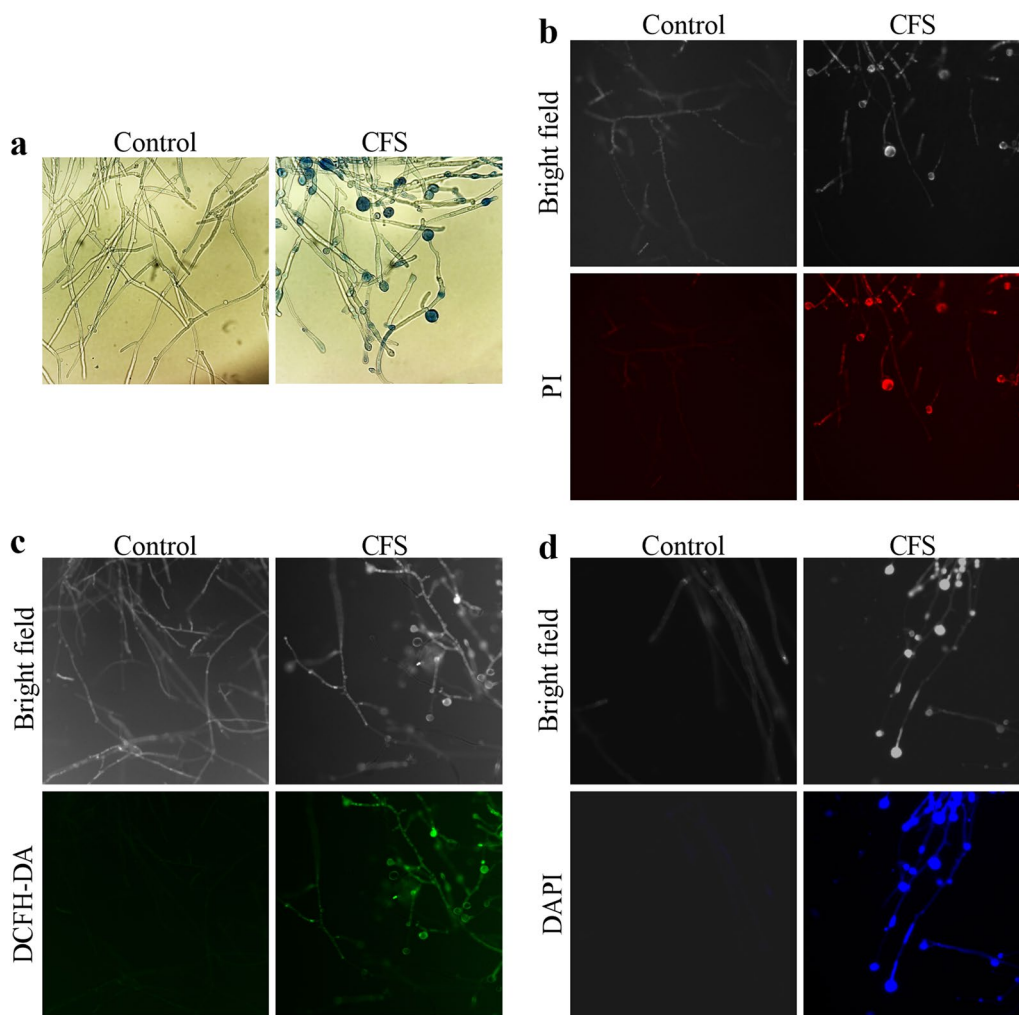
Fig. 5 Effect of compound fermentation supernatants (CFS) on mycelial cell of *Rhizoctonia cerealis*. **a** Effect of CFS on mycelial cell death; **b** Effect of CFS on cell membrane permeability. The fluorescence excitation wavelength is 536 nm; **c** Effect of CFS on ROS accumulation. The fluorescence excitation wavelength is 448 nm; **d** Effect of CFS on DNA damage. The fluorescence excitation wavelength is 340 nm

bacteria XZ20-1 and XZ38-3 were combined with *P. fluorescens* RB5, and the optimal ratio of the combination of three strains was quickly screened by the improved triangular coordinate diagram method. The final optimal ratio of the fermentation supernatants of antagonistic bacteria RB5, XZ20-1 and XZ38-3 was 2:6:4.

The successful use of a biocontrol agent depends upon being familiar with the biological environment in which the agent is to be used (Wang et al. 2020). The activity of antifungal products in the fermentation supernatants of antagonistic bacteria may be affected by different factors such as temperature, pH, ultraviolet light, and light (Hasani et al. 2018). Research has shown the inhibition

rate of *Streptomyces deccanensis* QY-3 fermentation supernatants remained more than 80% after high-temperature treatment at 100 °C for 1 h (Gu et al. 2020), and the relative inhibition rate of the compound fermentation supernatants (CFS) in this study was still 55.54% after 2 h treatment at 100 °C, indicating that the fermentation supernatants contained active substances that endure temperature. In addition, the CFS did not have a good tolerance to strong acid and alkali, and the suitable pH was 3–9, which was consistent with the results of intolerance in strong acids and bases in the fermentation supernatants of *Aspergillus* As-75 in the report of Jiang et al. (2019). Inhibitory rates of CFS were still higher than 55% when the ultraviolet light treatment time was longer

Yi *et al. Egyptian Journal of Biological Pest Control*   (2022) 32:121

Page 11 of 14

Fig. 6 Effects of fermentation supernatants of strains. **a** The distribution of disease levels of wheat sheath blight in each group; **b** Growth difference of wheats; **c** Plant height and root length of wheats; **d** Fresh and dry weight of wheats; **e** Chlorophylls a and chlorophylls b; **f** Carotenoid and protein; Different letters in the figures indicate significant differences ($P < 0.05$)

Table 3 Control efficacy of fermentation supernatants on wheat sheath blight

Treatment	Disease index (%)	Control efficacy (%)
CK	49.68[a]	–
RB5	27.75[b]	44.14 ± 3.82[c]
XZ20-1	19.84[c]	60.03 ± 4.40[b]
XZ38-3	24.60[bc]	50.53 ± 3.96[bc]
CFS	8.41[d]	83.05 ± 1.69[a]

Different letters in the same column indicate significant differences ($P < 0.05$)

than 90 min, which indicated CFS had better stability to ultraviolet light. When the fermentation supernatants were exposed to light for more than 6 h, their antifungal activity gradually decreased. But the inhibition rate was greater than 57% without significant changes, which indicated that the CFS had a strong tolerance to light, which agreed with sterile filtrates treated with illuminated light, and were stable in their activity against the pathogen (Yi et al. 2022a).

Yi *et al. Egyptian Journal of Biological Pest Control*   (2022) 32:121

Page 12 of 14

Biological control for plant pathogens is associated with the synthesis of bioactive substances, such as active protein, HCN and hydrolytic enzymes, considered as traits defining biocontrol ability (Liu et al. 2014). Zhang et al. (2020) purified an antifungal protein F_2 isolated from the culture supernatant of *B. subtilis* Z-14 against *R. cerealis*. *B. subtilis* V26 produced a variety of hydrolytic enzymes and volatile substances in the report of Ben Khedher et al. (2021). In the present study, *B. amyloliquefaciens* XZ20-1 and *B. velezensis* XZ38-3 could produce cellulase, protease, and amylase, while XZ20-1 produced more amylase and XZ38-3 produced more cellulase. Some metabolites produced from *Bacillus* can damage the pathogen cells and change the cell morphologies and structures or result in apoptosis and necrosis in a filamentous fungus such as *Rhizopus stolonifer* (Gong et al. 2015). Apoptosis involves multiple physiological changes in cells, including cell membrane damage, mitochondrial dysfunction and DNA fragmentation (Elmore 2007). ROS accumulation is a common response to fungal apoptosis (Zhang et al. 2021). Living cells have intact cell membrane, which can exclude some dyes, such as trypan blue, eosin, and PI, while dead cells do not have this ability. The study of Kim et al. (2017) indicated that the CLPs produced by *B. amyloliquefaciens* JCK-12 could change the cell membrane permeability of *F. graminearum* and produce strong antifungal activity. In this study, CFS can destroy the integrity of cell membrane, result in the destruction of DNA in *R. cerealis* and the death of mycelia, so CFS can be used to control wheat diseases caused by *R. cerealis*.

Xu et al. (2020) reported 5 strains of *Bacillus* and pig manure could control wheat sharp eye disease with the disease index decreased by 29.5% and the control efficacy reached 77.1%. In the present study, control efficacy of CFS was 83.05% and significantly higher than that of the single strain, which showed CFS had a profound biocontrol efficacy on wheat sheath blight. Many researchers have noticed that bacteria, such as *Pseudomonas*, *Azotobacter*, *Bacillus* and *Azospirillum* can promote plant growth through synergies (Kaki et al. 2013). Chlorophyll and carotenoid are the key elements for wheat leaves to convert light energy into chemical energy storage. Protein is the executor of various physiological functions and the embodiment of life phenomena. CFS treatment groups were significantly superior to the control group in plant height, root length, fresh weight, chlorophyll and soluble protein content. CFS could promote the synthesis of chlorophyll and soluble protein in wheat leaves, thereby increasing the light energy conversion rate and promoting wheat growth.

Conclusions

Antagonistic bacteria XZ20-1 and XZ38-3 were isolated and identified as *B. amyloliquefaciens* and *B. velezensis*, respectively, and they could produce cellulase, protease, amylase and siderophore. The optimal compound ratio (2:6:4) of fermentation supernatants of antagonistic strains (RB5, XZ20-1 and XZ38-3) can be quickly screened out through an improved triangle coordinate diagram method. Stability analysis showed CFS were relatively stable to pH, temperature, ultraviolet light and light. Compound fermentation supernatants (CFS) can cause cell membrane permeability changed, accumulation of ROS and DNA fragmentation. Moreover, CFS have good biocontrol effects and plant growth-promotion properties. This will provide a safe and efficient microbial control and growth promotion for wheat and have a potential for the development of microbial preparations.

Declarations

Author details
[1]School of Biological Engineering, Henan University of Technology, Zhengzhou 450001, China. [2]College of Life Science, Henan Agricultural University, Zhengzhou 450002, China. [3]The Key Laboratory of Functional Molecules for Biomedical Research, Zhengzhou 450001, China.

Yi *et al. Egyptian Journal of Biological Pest Control*   (2022) 32:121

Page 13 of 14

References

Ben Khedher S, Mejdoub-Trabelsi B, Tounsi S (2021) Biological potential of *Bacillus subtilis* V26 for the control of *Fusarium* wilt and tuber dry rot on potato caused by *Fusarium* species and the promotion of plant growth. Biol Control 152:104444. https://doi.org/10.1016/j.biocontrol.2020.104444

Carvalho A, Reis S, Pavia I, Lima-Brito JE (2019) Influence of seed priming with iron and/or zinc in the nucleolar activity and protein content of bread wheat. Protoplasma 256:763–775. https://doi.org/10.1007/s00709-018-01335-1

Dash BK, Rahman MM, Sarker PK (2015) Molecular identification of a newly isolated *Bacillus subtilis* BI19 and optimization of production conditions for enhanced production of extracellular amylase. Biomed Res Int 2015:859805. https://doi.org/10.1155/2015/859805

El-Helw NO, El-Gendy AO, El-Gebaly E, Hassan HM, Rateb ME, El-Nesr KA (2019) Characterization of natural bioactive compounds produced by isolated bacteria from compost of aromatic plants. J Appl Microbiol 126:443–451. https://doi.org/10.1111/jam.14085

Elmore S (2007) Apoptosis: a review of programmed cell death. Toxicol Pathol 35:495–516. https://doi.org/10.1080/01926230701320337

Gong AD, Li HP, Yuan QS, Song XS, Yao W, He WJ, Zhang JB, Liao YC (2015) Antagonistic mechanism of iturin A and plipastatin A from *Bacillus amyloliquefaciens* S76–3 from wheat spikes against *Fusarium graminearum*. PLoS ONE 10:e0116871. https://doi.org/10.1371/journal.pone.0116871

Gu LS, Zhang K, Zhang N, Li XY, Liu ZQ (2020) Control of the rubber anthracnose fungus *Colletotrichum gloeosporioides* using culture filtratio extract from *Streptomyces deccanensis* QY-3. Antonie Van Leeuwenhoek 113:1573–1585. https://doi.org/10.1007/s10482-020-01465-8

Guerrero R (2001) Bergey's manuals and the classification of prokaryotes. Int Microbiol 4:103–109. https://doi.org/10.1007/s101230100021

Guo LD, Hyde KD, Liew ECY (2000) Identification of endophytic fungi from *Livistona chinensis* based on morphology and rDNA sequences. New Phytol 147:617–630. https://doi.org/10.1046/j.1469-8137.2000.00716.x

Hasan N, Farzand A, Heng Z, Khan IU, Moosa A, Zubair M, Na Y, Ying S, Canming T (2020) Antagonistic potential of novel endophytic *Bacillus strains* and mediation of plant defense against Verticillium wilt in upland cotton. Plants (basel) 9:1438. https://doi.org/10.3390/plants9111438

Hasani ZP, Moghimi H, Hamedi J (2018) Biosurfactant production by *Mucor circinelloides*: environmental applications and surface-active properties. Eng Life Sci 18:317–325. https://doi.org/10.1002/elsc.201700149

Helepciuc FE, Todor A (2021) EU microbial pest control: a revolution in waiting. Pest Manag Sci. https://doi.org/10.1002/ps.6721

Hu CH, Ren LQ, Zhou Y, Ye BC (2019) Characterization of antifungal activity of three *Lactobacillus plantarum* strains isolated from Chinese traditional dairy food. Food Sci Nutr 7:1997–2005. https://doi.org/10.1002/fsn3.1025

Jiang B, Wang ZY, Xu CX, Liu WJ, Jiang DH (2019) Screening and identification of *Aspergillus* activity against *Xanthomonas oryzae* pv. oryzae and analysis of antifungal components. J Microbiol 57:597–605. https://doi.org/10.1007/s12275-019-8330-5

Kaki AA, Chaouche N, Dehimat L, Milet A, Youcef-Ali M, Ongena M, Thonart P (2013) Biocontrol and plant growth promotion characterization of *Bacillus* species isolated from *Calendula officinalis* rhizosphere. Indian J Microbiol 53:447–452. https://doi.org/10.1007/s12088-013-0395-y

Kim K, Lee Y, Ha A, Kim JI, Park AR, Yu NH, Son H, Choi GJ, Park HW, Lee CW, Lee T, Lee YW, Kim JC (2017) Chemosensitization of *Fusarium graminearum* to chemical fungicides using cyclic lipopeptides produced by *Bacillus amyloliquefaciens* strain JCK-12. Front Plant Sci 8:2010. https://doi.org/10.3389/fpls.2017.02010

Kulišová M, Vrublevskaya M, Lovecká P, Vrchotová B, Stránská M, Kolařík M, Kolouchová I (2021) Fungal endophytes of *Vitis vinifera*—plant growth promotion factors. Agriculture 11:1250. https://doi.org/10.3390/agriculture11121250

Kumar S, Stecher G, Tamura K (2016) MEGA7: molecular evolutionary genetics analysis version 7.0 for bigger datasets. Mol Biol Evol 33:1870–1874. https://doi.org/10.1093/molbev/msw054

Li SF, Zhang SB, Zhai HC, Lv YY, Hu YS, Cai JP (2021) Hexanal induces early apoptosis of *Aspergillus flavus* conidia by disrupting mitochondrial function and expression of key genes. Appl Microbiol Biotechnol 105:6871–6886. https://doi.org/10.1007/s00253-021-11543-0

Lichtenthaler HK, Wellburn AR (1983) Determinations of total carotenoids and chlorophylls a and b of leaf extracts in different solvents. Biochem Soc Trans 11:591–592

Lim SM, Yoon MY, Choi GJ, Choi YH, Jang KS, Shin TS, Park HW, Yu NH, Kim YH, Kim JC (2017) Diffusible and volatile antifungal compounds produced by an antagonistic *Bacillus velezensis* G341 against various phytopathogenic fungi. Plant Pathol J 33:488–498. https://doi.org/10.5423/PPJ.OA.04.2017.0073

Liu Y, Lai QL, Dong CM, Sun FQ, Wang LP, Li GY, Shao ZZ (2013) Phylogenetic diversity of the *Bacillus pumilus* group and the marine ecotype revealed by multilocus sequence analysis. PLoS ONE 8:e80097. https://doi.org/10.1371/journal.pone.0080097

Liu JJ, Hagberg I, Novitsky L, Hadj-Moussa H, Avis TJ (2014) Interaction of antimicrobial cyclic lipopeptides from *Bacillus subtilis* influences their effect on spore germination and membrane permeability in fungal plant pathogens. Fungal Biol 118:855–861. https://doi.org/10.1016/j.funbio.2014.07.004

Ma ZW, Hua GKH, Ongena M, Höfte M (2016) Role of phenazines and cyclic lipopeptides produced by *Pseudomonas* sp. CMR12a in induced systemic resistance on rice and bean. Environ Microbiol Rep 8:896–904. https://doi.org/10.1111/1758-2229.12454

Miller GL (1959) Use of dinitrosalicylic acid reagent for determination of reducing sugar. Anal Chem 31:426–428

Nassar R, Kamel HA, Ghoniem AE, Alarcon JJ, Sekara A, Ulrichs C, Abdelhamid MT (2020) Physiological and anatomical mechanisms in wheat to cope with salt stress induced by seawater. Plants (basel) 9:237. https://doi.org/10.3390/plants9020237

Nguyen HTT, Choi S, Kim S, Lee JH, Park AR, Yu NH, Yoon H, Bae CH, Yeo JH, Choi GJ, Son H, Kim JC (2020) The hsp90 inhibitor, monorden, Is a promising lead compound for the development of novel fungicides. Front Plant Sci 11:371. https://doi.org/10.3389/fpls.2020.00371

Niu B, Wang WX, Yuan ZB, Sederoff RR, Sederoff H, Chiang VL, Borriss R (2020) Microbial interactions within multiple-strain biological control agents impact soil-borne plant disease. Front Microbiol 11:585404. https://doi.org/10.3389/fmicb.2020.585404

Pan ZX, Munir S, Li YM, He PB, He PF, Wu YX, Xie Y, Fu ZW, Cai YZ, He YQ (2021) Deciphering the *Bacillus amyloliquefaciens* B9601–Y2 as a potential antagonist of tobacco leaf mildew pathogen during flue-curing. Front Microbiol 12:683365. https://doi.org/10.3389/fmicb.2021.683365

Peng D, Li SD, Chen CJ, Zhou MG (2014) Combined application of *Bacillus subtilis* NJ-18 with fungicides for control of sheath blight of wheat. Biol Control 70:28–34. https://doi.org/10.1016/j.biocontrol.2013.11.013

Ren Y, Yu PB, Wang Y, Hou WX, Yang X, Fan JL, Wu XH, Lv XL, Zhang N, Zhao L, Dong ZD, Chen F (2020) Development of a rapid approach for detecting sheath blight resistance in seedling-stage wheat and its application in Chinese wheat cultivars. Plant Dis 104:1662–1667. https://doi.org/10.1094/PDIS-12-19-2718-RE

Sofue M, Ueda Y, Yamamoto M, Yamasaki T, Manabe T (1997) Determination of formulation quantities for three kinds of antacid using triangle coordinates. Yakugaku Zasshi J Pharm Soc Jpn 117:185–192. https://doi.org/10.1248/yakushi1947.117.3_185

Su Q, Wang K, Zhang ZY (2020) Ecotopic expression of the antimicrobial peptide DmAMP1W improves resistance of transgenic wheat to two diseases: sheath blight and common root rot. Int J Mol Sci 21:647. https://doi.org/10.3390/ijms21020647

Su J, Zhao JJ, Zhao SQ, Li MY, Pang SY, Kang ZS, Zhen WC, Chen SS, Chen F, Wang XD (2021) Genetics of resistance to common root rot (Spot blotch), *Fusarium crown* rot, and sheath blight in wheat. Front Genet 12:699342. https://doi.org/10.3389/fgene.2021.699342

Tian PP, Lv YY, Lv A, Yuan WJ, Zhang SB, Li N, Hu YS (2021) Antifungal effects of fusion puroindoline B on the surface and intracellular environment of *Aspergillus flavus*. Probiotics Antimicrob Proteins 13:249–260. https://doi.org/10.1007/s12602-020-09667-2

Wang XY, Zhou XN, Cai ZB, Guo L, Chen XL, Chen X, Liu JY, Feng MF, Qiu YW, Zhang Y, Wang A (2020) A biocontrol strain of *Pseudomonas aeruginosa* CQ-40 promote growth and control *Botrytis cinerea* in tomato. Pathogens 10:22. https://doi.org/10.3390/pathogens10010022

WoldemariamYohannes K, Wan Z, Yu QL, Li HY, Wei XT, Liu YL, Wang J, Sun BG (2020) Prebiotic, antagonistic, antimicrobial, and functional food

applications of *Bacillus amyloliquefaciens*. J Agric Food Chem 68:14709–14727. https://doi.org/10.1021/acs.jafc.0c06396

Xu YB, Chen M, Zhang Y, Wang M, Wang Y, Huang QB, Wang X, Wang G (2014) The phosphotransferase system gene ptsI in the endophytic bacterium *Bacillus cereus* is required for biofilm formation, colonization, and biocontrol against wheat sheath blight. FEMS Microbiol Lett 354:142–152. https://doi.org/10.1111/1574-6968.12438

Xu YL, Li XY, Cong C, Gong GL, Xu YP, Che J, Hou FQ, Chen HL, Wang LL (2020) Use of resistant *Rhizoctonia cerealis* strains to control wheat sheath blight using organically developed pig manure fertilizer. Sci Total Environ 726:138568. https://doi.org/10.1016/j.scitotenv.2020.138568

Yi YL, Li ZB, Song CX, Kuipers OP (2018) Exploring plant-microbe interactions of the rhizobacteria *Bacillus subtilis* and *Bacillus mycoides* by use of the CRISPR-Cas9 system. Environ Microbiol 20:4245–4260. https://doi.org/10.1111/1462-2920.14305

Yi YJ, Luan PY, Liu SF, Shan YT, Hou ZP, Zhao SY, Jia S, Li RF (2022a) Efficacy of *Bacillus subtilis* XZ18-3 as a biocontrol agent against *Rhizoctonia cerealis* on wheat. Agriculture 12:258. https://doi.org/10.3390/agriculture12020258

Yi YJ, Luan PY, Wang K, Li GL, Yin YN, Yang YH, Zhang QY, Liu Y (2022b) Antifungal activity and plant growth-promotion properties of *Bacillus mojovensis* B1302 against *Rhizoctonia cerealis*. Microorganisms 10:1682. https://doi.org/10.3390/microorganisms10081682

Zhang ZX, Wang HY, Wang KY, Jiang LL, Wang D (2017) Use of lentinan to control Sharp eyespot of wheat, and the mechanism involved. J Agric Food Chem 65:10891–10898. https://doi.org/10.1021/acs.jafc.7b04665

Zhang XC, Guo XJ, Wu CH, Li CC, Zhang DD, Zhu BC (2020) Isolation, heterologous expression, and purification of a novel antifungal protein from *Bacillus subtilis* strain Z-14. Microb Cell Fact 19:214. https://doi.org/10.1186/s12934-020-01475-1

Zhang SB, Qin YL, Li SF, Lv YY, Zhai HC, Hu YS, Cai JP (2021) Antifungal mechanism of 1-nonanol against *Aspergillus flavus* growth revealed by metabolomic analyses. Appl Microbiol Biotechnol 105:7871–7888. https://doi.org/10.1007/s00253-021-11581-8

Zhao SS, Zhang YY, Yan W, Cao LL, Xiao Y, Ye YH (2017) *Chaetomium globosum* CDW7, a potential biological control strain and its antifungal metabolites. FEMS Microbiol Lett 364:1–6. https://doi.org/10.1093/femsle/fnw287

Publisher's Note